Robotica (2001) volume 19, pp. 601–610. Printed in the United Kingdom © 2001 Cambridge University Press

Real-Time Motion Capture for a Human Body using Accelerometers*

Jihong Lee and Insoo Ha

Dept. of Mechatronics Engineering, Chung-nam University, 220 Kung-dong, Yusong-gu, Taejon, 305-764 (Korea)
e-mail: jihong@cnu.chungnam.ac.kr

(Received in Final Form: 19 December, 2000)

SUMMARY

In this paper we propose a set of techniques for a real-time motion capture of a human body. The proposed motion capture system is based on low cost accelerometers, and is capable of identifying the body configuration by extracting gravity-related terms from the sensor data. One sensor unit is composed of 3 accelerometers arranged orthogonally to each other, and is capable of identifying 2 rotating angles of joints with 2 degrees of freedom. A geometric fusion technique is applied to cope with the uncertainty of sensor data. A practical calibration technique is also proposed to handle errors in aligning the sensing axis to the coordination axis. In the case where motion acceleration is not negligible compared with gravity acceleration, a compensation technique to extract gravity acceleration from the sensor data is proposed. Experimental results not only for individual techniques but also for human motion capturing with graphics are included.

KEYWORDS: Accelerometers; Real-time motion; Human body; Sensors

1. INTRODUCTION

Motion capture is a technique that interfaces information about the motion of a human body or mechanical body with computer systems. Motion capture is applied in the fields of virtual reality, simulation, entertainment, medical and biomechanical usage. Widely used methods of motion capture are based on the electromagnetic technique or the optical technique. The electromagnetic method suffers from problems such as magnetic interference from surrounding metals, difficult calibration and intrinsic noise. The optical method suffers from such problems since its performance is strongly affected by illumination, and it cannot be used in real-time applications since it requires post-processing of data to extract information of motion. Moreover, commercially available products adopting these kinds of techniques are currently too expensive to be used by general users.

The system is equiped with multiple sensors, and therefore can offer high-level adaptability for uncertain environments.[1] There are, however, some nonindustrial tasks where attaching internal sensors is not possible. Motion capture of a human body may be one example of these tasks. Due to the uncertainties, these kind of tasks require more and more sensors to identify motions.

In this paper we propose a cost-effective motion capture technique, which is based on low cost accelerometers. The technique implements a real-time connection between sensing and motion. Each sensor unit of the system is composed of 3 accelerometers that are arranged orthogonally to each other. The sensor unit measures acceleration along each sensor and is capable of identifying 2 joint angles of a mechanical system which have 2 degrees of freedom. To transform the sensor information to a human body configuration, we model the body into several open loop kinematic chains. After that, we attach one sensor unit to each link having 2 degrees of freedom, as well as special purpose sensors such as electromagnetic compasses and gyro sensors.

The main contributions of this paper are to introduce low cost accelerometers to human body motion capture and to develop mathematical relations between the sensor data and the human body configurations. Other contributions include techniques to overcome the problems encountered when applying this low cost sensor system to motion capture. The problems mentioned above include; intrinsic uncertainties of the sensors, calibration of the sensor system to transform the sensor data to motion space and decomposing the acceleration data into gravity term and motion term.

To overcome the intrinsic uncertainties in sensor data, we apply geometric optimization for sensor fusion[2–4] to the information processing. Sensor fusion is a technology which to extracts more reliable information from multiple sensors.[5,6] By applying the fusion technique, can we improve the estimation of the sensor information. Our results show that sensor information has a smaller variance using this kind of processing.

Even though the variances of the sensor information are reduced through sensor fusion, the mean value of the information is strongly dependent on the calibration of the sensor system. Therefore, we also propose a calibration method to make the sensor information approach the real value. The calibration starts from the process that determines the tilting angles of each sensor axis from the corresponding coordination axis. The tilting angles between the coordination axis and the sensor axis are summarized in an error matrix. After correcting the sensor information through the error matrix, we obtain results that are closer to the real values.

* This work was supported by Institute of Information Technology Assessment of Korea.

https://doi.org/10.1017/S0263574701003319 Published online by Cambridge University Press

Since integrating the sensor data to get rotating angles often causes unstable results, the method proposed in this paper is only based on gravity acceleration. The measured data includes both motion acceleration and gravity acceleration. When the motion components are too large to be ignored, we have to decompose the gravity component and motion component from the measured sensor data. We propose a technique that decomposes the two components by using redundant sensor units. Experimental results for a simple 1 degree of freedom system are included in this paper.

In Section 2, we briefly describe the capture system. Basic theory for multiple sensor fusion and some results are summarized in Section 3 where we will apply the geometric sensor fusion theory to identify 2 joint angles. In Section 4, the calibration technique for the proposed sensor system is introduced. Decomposing gravity acceleration and motion acceleration from sensor data is described in Section 5. Several examples of capturing human body motion are illustrated in Section 6, while a brief summary of this work is given in Section 7.

2. SYSTEM CONFIGURATION

2.1. System overview

The type of accelerometer used in this experiment is the ADXL05 manufactured by Analog Devices. The sensors are known to be fabricated by MEMS technology and have range from 1 g(gravity acceleration) to 5 g, according to external circuits. The layout of the sensor system including ADXL05 and supplementary circuits is shown in Figure 1, and the whole system is described in Figure 2. The overall system is composed of sensor systems, an interface system (Lab-PC 1200, National Instrument) and a computer for data processing and display. We sample the motion data up to 1,000 samples per second and animate the simplified character (developed in OpenGL-based system) 30 frames per second. The system acquires sensory data (acceleration data), extracts sensory information (joint angles) from the sensory data, performs necessary data processing and displays the character on a computer monitor.

Since one accelerometer senses acceleration along one direction, we combine three sensors so that each sensor axis is orthogonal to each other. The acceleration of a mechanical body has two different components; acceleration by gravity and acceleration by motion itself. Let $\boldsymbol{\theta}_g$ and $\boldsymbol{\theta}_a$ be acceleration components of gravity and motion, respectively. Then, the output of a sensor $\boldsymbol{\theta}$ is described by

$$\boldsymbol{\theta} = \boldsymbol{\theta}_t + \boldsymbol{\theta}_a \tag{1}$$

Here, we assume that $\boldsymbol{\theta}_g \gg \boldsymbol{\theta}_a$, say, the motions is not so highly accelerated or decelerated compared with gravity. Then, we, obtain

$$\boldsymbol{\theta} \approx \boldsymbol{\theta}_g \tag{2}$$



Fig. 1. ADXL50 accelerometer and supplementary circuit.

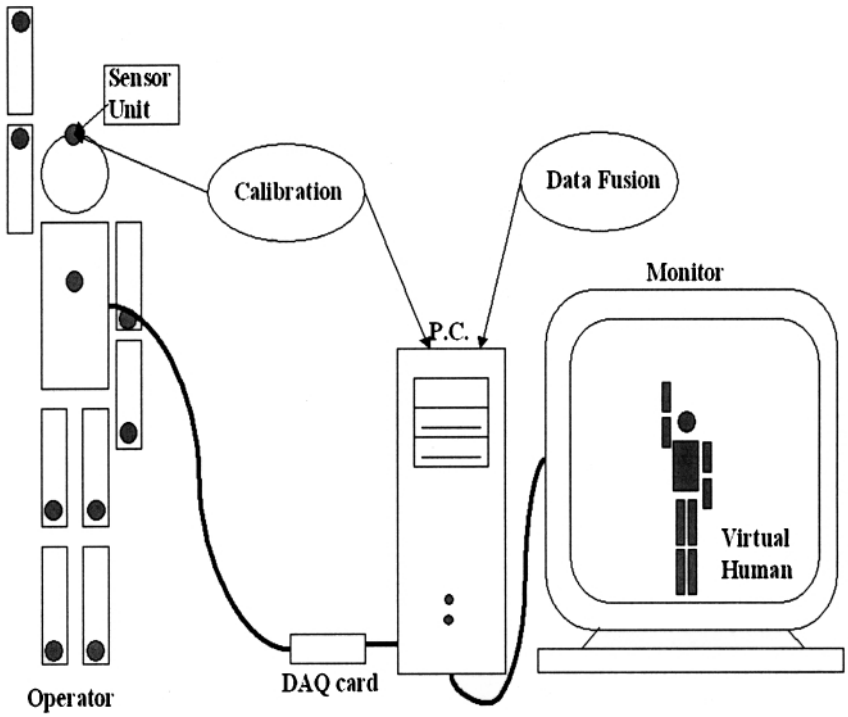


Fig. 2. Overall structure of the real-time motion capturing system.

https://doi.org/10.1017/S0263574701003319 Published online by Cambridge University Press

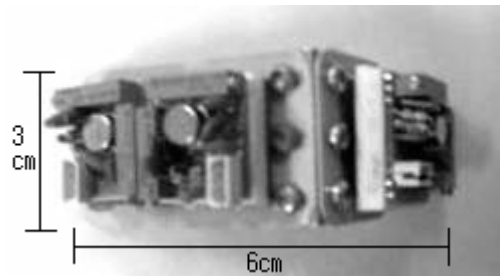


Fig. 3. A sensor unit composed of 3 accelerometers. One sensor unit is as heavy as 5 grams.

2.2. Sensor unit

The basic components of the sensor system are three accelerometers shown in Figure 3. The three sensors placed orthogonally to each other make up the sensor unit. The sensor unit is attached to a virtual link having two degrees of freedom as in Figure 4. Let the two rotating angles of the joints be α and β. Then the coordinate transformation of the sensor unit is described as follows:

$$\boldsymbol{G}_{\alpha,\beta} \equiv \boldsymbol{R}_{x,\alpha}\boldsymbol{R}_{x,\beta} \tag{3}$$

$$= \begin{bmatrix} \cos\alpha & -\sin\alpha & 0 \\ \sin\alpha & \cos\alpha & 0 \\ 0 & 0 & 1 \end{bmatrix} \cdot \begin{bmatrix} 1 & 0 & 0 \\ 0 & \cos\beta & -\sin\beta \\ 0 & \sin\beta & \cos\beta \end{bmatrix} \tag{4}$$

$$= \begin{bmatrix} \cos\alpha & -\sin\alpha\cos\beta & \sin\alpha\sin\beta \\ \sin\alpha & \cos\alpha\cos\beta & -\cos\alpha\sin\beta \\ 0 & \sin\beta & \cos\beta \end{bmatrix} \equiv [\boldsymbol{G}_x \boldsymbol{G}_y \boldsymbol{G}_z] \tag{5}$$

Assuming that the axis of gravity $\boldsymbol{g}$ is aligned to $\boldsymbol{y}_0$, we connect the sensor data and the coordination as:

$$\boldsymbol{G}_x \cdot (\boldsymbol{g}) = \sin\alpha = \theta_x \tag{6}$$

$$\boldsymbol{G}_y \cdot (\boldsymbol{g}) = \cos\alpha\cos\beta = \theta_y \tag{7}$$

$$\boldsymbol{G}_z \cdot (\boldsymbol{g}) = -\cos\alpha\sin\beta = \theta_z \tag{8}$$

The above equation can be represented in matrix form as:

$$\boldsymbol{G}^T_{\alpha,\beta}(\boldsymbol{g}) = [\theta_x \;\; \theta_y \;\; \theta_z] \tag{9}$$

From (6) through (8), we get the following equations for the rotating angles:

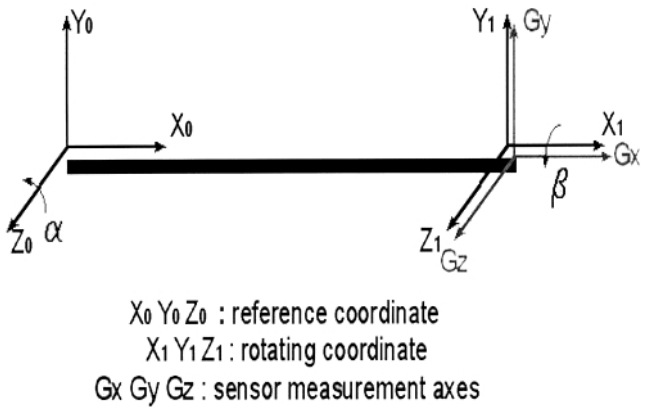


Fig. 4. Coordinate system of the sensor unit attached to virtual link.

$$\alpha = tan^{-1}\left(\frac{\theta_x \cos\beta}{\theta_y}\right) \tag{10}$$

$$\beta = tan^{-1}\left(-\frac{\theta_z}{\theta_y}\right) \tag{11}$$

Note that the above equations are based on the assumption that three sensors are aligned orthogonal to each other. The errors in the alignment will be handled later

3. GEOMETRIC SENSOR FUSION

3.1. Basic theory

Here, we briefly summarize the geometric sensor fusion based on the previous research results.[3] Let $\boldsymbol{\theta}^i \in R^m$, $i = 1, 2, \ldots, p$ be sensory data from sensor unit i, and $\boldsymbol{x}^i \in R^n$, $i = 1, 2, \ldots, p$ be sensory information that is computed from $\boldsymbol{\theta}^i$ as:

$$\boldsymbol{x}^i = f^i(\boldsymbol{\theta}^i). \tag{12}$$

The uncertainty included in the sensory data is assumed additive and represented as follows:

$$\boldsymbol{\theta}^i = \underline{\boldsymbol{\theta}^i} + \delta\boldsymbol{\theta}^i \tag{13}$$

where $\delta\boldsymbol{\theta}^i \in R^{m_i}$ is the uncertainty and $\underline{\boldsymbol{\theta}^i}$ is the expected value.

Assuming a Gaussian distribution for $\delta\boldsymbol{\theta}^i$ and denoting its covariance matrix as $\boldsymbol{Q}^i$, we expand the following equation with linear approximation:

$$\begin{aligned} \boldsymbol{x}^i &= f^i(\underline{\boldsymbol{\theta}^i} + \delta\boldsymbol{\theta}^i) \\ &\approx f^i(\underline{\boldsymbol{\theta}^i}) + J^i(\boldsymbol{\theta}^i)\delta\boldsymbol{\theta}^i \end{aligned} \tag{14}$$

where

$$J^i(\boldsymbol{\theta}^i) = \frac{\partial f^i}{\partial \boldsymbol{\theta}^i} \in R^{n \times m_i}. \tag{15}$$

Then, the mean and covariance of $\boldsymbol{x}^i$ become

$$\boldsymbol{x}^i \equiv \vec{\boldsymbol{x}^i} = f^i(\underline{\boldsymbol{\theta}^i}) \tag{16}$$

$$\begin{aligned} V[\boldsymbol{x}^i] &\equiv E[(\boldsymbol{x}^i - \vec{\boldsymbol{x}^i})(\boldsymbol{x}^i - \vec{\boldsymbol{x}^i})^T] \\ &= E[\boldsymbol{J}^i \delta\boldsymbol{\theta}^i \delta\boldsymbol{\theta}^{i^T} \; \boldsymbol{J}^{i^T}] \\ &= \boldsymbol{J}^i \boldsymbol{Q}^i \boldsymbol{J}^{i^T} \end{aligned} \tag{17}$$

The optimal linear combination of the sensory information is calculated as follows:

$$\boldsymbol{x} = \sum_{i=1}^{p} \boldsymbol{W}^i \boldsymbol{x}^i \tag{18}$$

$$\boldsymbol{W}^i = \left\{ \sum_{i=1}^{p} (\boldsymbol{J}^i \boldsymbol{Q}^i \boldsymbol{J}^{i^T})^{-1} \right\}^{-1} (\boldsymbol{J}^i \boldsymbol{Q}^i \boldsymbol{J}^{i^T})^{-1} \tag{19}$$

https://doi.org/10.1017/S0263574701003319 Published online by Cambridge University Press

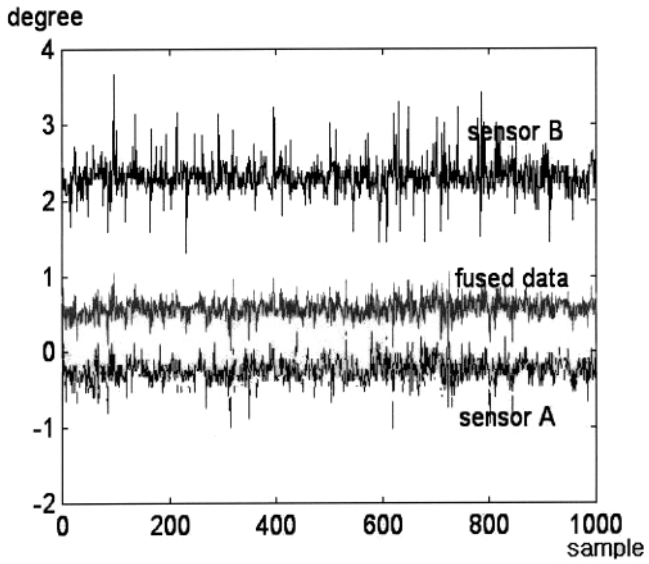


Fig. 5. The effect of fusion for the sensor information α. The experiments were performed with true $\alpha=0$.

3.2 Experimental results

We apply the geometric sensor fusion technique to the case shown in Figure 4. Two sensor units (i.e., 6 accelerometers) give sensory data in order to get 2-dimensional sensor information $\boldsymbol{x}=[\alpha\ \ \beta]^T$. The fusion results for joint angle α are shown in Figure 5, while covariances for both α and β after 1000 samples are shown in Table I.

In the result, we study three cases: $[\alpha\ \ \beta]=[0\ \ 0]$ degree, $[\alpha\ \ \beta]=[20\ \ 0]$ degree, and $[\alpha\ \ \beta]=[50\ \ 0]$ degree. As shown in the results, the uncertainty represented as the covariance of $\boldsymbol{x}$ is reduced maximally 5 times, while the mean value is not improved dramatically. After some analysis we concluded that the error in mean value is caused by a calibration error (i.e. an error in the assumption that the three sensor axes are orthogonal to each other). We will handle this calibration later.

4. CALIBRATION

As described before, the calibration plays a crucial role in making the sensory information approach the true value. When we combine the 3 sensors to compose one sensor unit, we try to align each sensor axis to one of the coordination axes. However, some errors may arise when aligning the sensor axis to the coordination axis (See Figure 6).

Consulting Figure 4, we connect the sensor data and the coordination axis as follows:

$$\boldsymbol{G}_{\alpha,\beta}^{T}\boldsymbol{g}=[\boldsymbol{\theta}_x\ \ \boldsymbol{\theta}_y\ \ \boldsymbol{\theta}_z]^T \tag{20}$$

Table I. Covariances of two sensor information from sensor unit A, sensor unit B, and fused information.

	$[\alpha\ \ \beta]=[0\ \ 0]$		$[\alpha\ \ \beta]=[20\ \ 0]$		$[\alpha\ \ \beta]=[50\ \ 0]$	
	$V(\alpha)$	$V(\beta)$	$V(\alpha)$	$V(\beta)$	$V(\alpha)$	$V(\beta)$
unit A	0.0510	0.0207	0.0396	0.0215	0.0279	0.0537
unit B	0.0250	0.0884	0.0286	0.0836	0.0400	0.1586
fused result	0.0170	0.0169	0.0182	0.0196	0.0400	0.1586

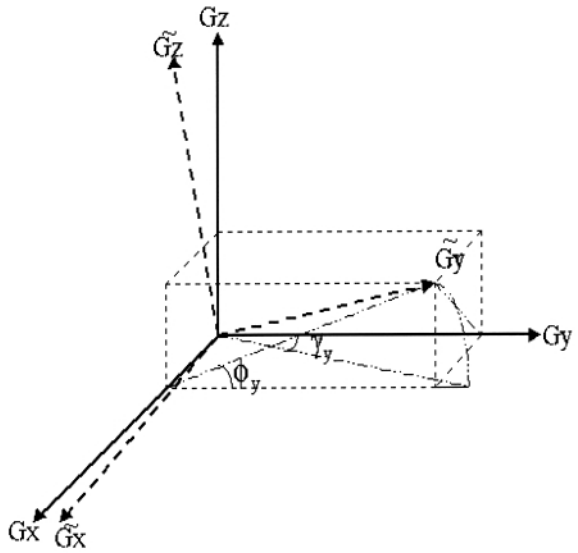


Fig. 6. Alignment error in sensor coordination axis.

Each sensor axis with respect to base coordinate is described as follows:

$$(\boldsymbol{G}_{\alpha,\beta}\boldsymbol{R}_{y,\phi_x}\boldsymbol{R}_{z,\gamma_x})^T\boldsymbol{x}_0=\bar{\boldsymbol{G}}_x \tag{21}$$

$$(\boldsymbol{G}_{\alpha,\beta}\boldsymbol{R}_{x,\phi_y}\boldsymbol{R}_{z,\gamma_y})^T\boldsymbol{y}_0=\bar{\boldsymbol{G}}_y \tag{22}$$

$$(\boldsymbol{G}_{\alpha,\beta}\boldsymbol{R}_{x,\phi_z}\boldsymbol{R}_{y,\gamma_z})^T\boldsymbol{z}_0=\bar{\boldsymbol{G}}_z \tag{23}$$

Since

$$(\boldsymbol{G}_{\alpha,\beta}\boldsymbol{\Psi}_{sensor})^T\boldsymbol{g}=[\tilde{\boldsymbol{\theta}}_x\ \ \tilde{\boldsymbol{\theta}}_y\ \ \tilde{\boldsymbol{\theta}}_z]^T \tag{24}$$

$$\boldsymbol{\Psi}_{sensor}=[(\boldsymbol{R}_{y,\phi_x}\boldsymbol{R}_{z,\gamma_x})\boldsymbol{x}_0(\boldsymbol{R}_{x,\phi_y}\boldsymbol{R}_{z,\gamma_y})\boldsymbol{y}_0(\boldsymbol{R}_{x,\phi_z}\boldsymbol{R}_{y,\gamma_x})\boldsymbol{z}_0] \tag{25}$$

from (20) and (24) we get

$$[\boldsymbol{\theta}_x\ \ \boldsymbol{\theta}_y\ \ \boldsymbol{\theta}_z]=[\tilde{\boldsymbol{\theta}}_x\ \ \tilde{\boldsymbol{\theta}}_y\ \ \tilde{\boldsymbol{\theta}}_z]\boldsymbol{\Psi}_{sensor}^{-1} \tag{26}$$

The $\boldsymbol{\Psi}_{sensor}$ can be measured with specifically designed robot-like devices. By applying calculated $[\boldsymbol{\theta}_x\ \ \boldsymbol{\theta}_y\ \ \boldsymbol{\theta}_z]$ instead of $[\tilde{\boldsymbol{\theta}}_x\ \ \tilde{\boldsymbol{\theta}}_y\ \ \tilde{\boldsymbol{\theta}}_z]$ in calculating joint angle α and β, we get better results as shown in Figure 7. The true α is 30

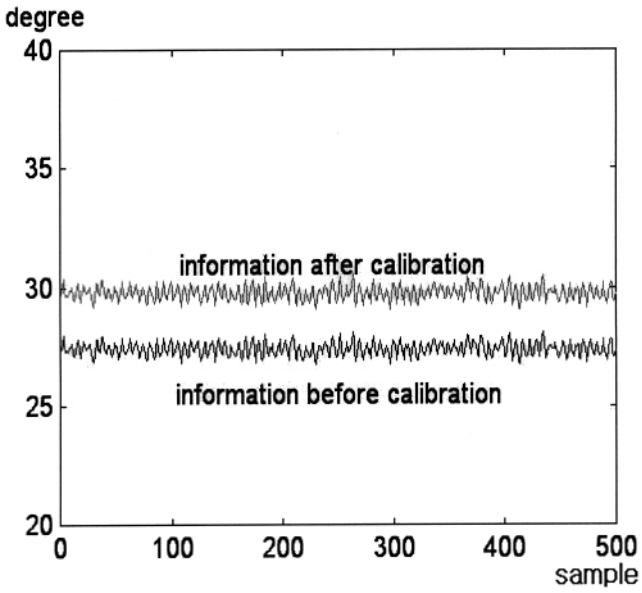


Fig. 7. Effect of calibration in calculating joint angle.

https://doi.org/10.1017/S0263574701003319 Published online by Cambridge University Press

degrees in this case, and the result shows that the calculated joint angle α approaches the true value through calibration.

When we attach the sensor unit to a human body after the calibration described above, some additional expected errors are described as:

$$(\boldsymbol{G}_{\alpha,\beta}\boldsymbol{R}_{attach}\boldsymbol{\Psi}_{sensor})^T\boldsymbol{y}=[\tilde{\theta}_x \;\; \tilde{\theta}_y \;\; \tilde{\theta}_z]^T \tag{27}$$

$$\boldsymbol{R}_{attach}=\boldsymbol{R}_{\theta,\psi,\lambda} \tag{28}$$

The identification of this rotation matrix will be included in future research work.

5. COMPENSATION FOR FAST MOTIONS

As mentioned before, the sensor data contain two kinds of acceleration; one from gravity and the other from accelerational motion of body. In the case where accelerational motion is no more negligible. (i.e., the case where the assumption $\boldsymbol{\theta}_g \gg \boldsymbol{\theta}_a$, does not hold any more) the method based only on gravity cannot capture the body configuration exactly. We need a technique so that we may handle this case in a proper manner.

Assuming rotational motions, the accelerational relation between adjacent links are described as the following:[7]

$$\dot{\boldsymbol{v}}_i=\dot{\boldsymbol{w}}_i\times\boldsymbol{p}_i^*+\boldsymbol{w}_i\times(\boldsymbol{w}_i\times\boldsymbol{p}_i^*)+\dot{\boldsymbol{v}}_{i-1} \tag{29}$$

where

$\boldsymbol{v}_i$ = linear velocity of i th coordinate frame,
$\dot{\boldsymbol{w}}_i$ = angular acceleration of i th coordinate frame,
$\boldsymbol{w}_i$ = angular velocity of i th coordinate frame, and
$\boldsymbol{p}_i^*$ = the origin of the ith coordinate frame with respect to the $(i-1)$th coordinate system.

The first term is the linear acceleration term, the second is a Coliolis and Centrifugal motion-related term, and the last reflects the previous link's acceleration. Note $\dot{\boldsymbol{v}}_0=\boldsymbol{g}=[0 \;\; 0 \;\; -9.8 m/sec^2]^T$. The above representation is based on the Netwon-Euler formula expressed about a base coordinate frame. Since each accelerometer is, however, attached to a moving body, its output data should be represented with respect to its own coordinate frame. So we re-describe equation (29) in the following forms:

$$\begin{aligned}{}^i\boldsymbol{R}_0\dot{\boldsymbol{v}}_i=&({}^i\boldsymbol{R}_0\dot{\boldsymbol{w}}_i)\times({}^i\boldsymbol{R}_0\boldsymbol{p}_i^*)+({}^i\boldsymbol{R}_0\boldsymbol{w}_i)\times[({}^i\boldsymbol{R}_0\boldsymbol{w}_i)\times({}^i\boldsymbol{R}_0\boldsymbol{p}_i^*)]\\&+{}^i\boldsymbol{R}_{i-1}({}^{i-1}\boldsymbol{R}_0\dot{\boldsymbol{v}}_{i-1})\end{aligned} \tag{30}$$

where ${}^i\boldsymbol{R}_j$ is the coordiante transformation matrix from i to j.

According to equation (30), we know the first two terms are dependent on link geometry (p_i^*) while the last term is not. Utilizing this property, we can extract the rotational angles of a moving body from multiple sensor units. For the two sensor systems attached at link i shown in Figure 9, we assume that the geometry of the attached sensor systems with respect to the $(i-1)$th coordinate system are known. Then, we can transform the measured senor data along the sensing axes into the data represented with respect to the $(i-1)$th coordinate system. We describe the transformed acceleration as:

$$\begin{aligned}{}^i\boldsymbol{R}_0\bar{\boldsymbol{a}}_i^A=&({}^i\boldsymbol{R}_0\dot{\boldsymbol{w}}_i)\times({}^i\boldsymbol{R}_0\bar{\boldsymbol{s}}_i^A)+({}^i\boldsymbol{R}_0\boldsymbol{w}_i)\times[({}^i\boldsymbol{R}_0\boldsymbol{w}_i)\times({}^i\boldsymbol{R}_0\bar{\boldsymbol{s}}_i^A)]\\&+{}^i\boldsymbol{R}_0\dot{\boldsymbol{v}}_{i-1}\end{aligned} \tag{31}$$

$$\begin{aligned}{}^i\boldsymbol{R}_0\bar{\boldsymbol{a}}_i^B=&({}^i\boldsymbol{R}_0\dot{\boldsymbol{w}}_i)\times({}^i\boldsymbol{R}_0\bar{\boldsymbol{s}}_i^B)+({}^i\boldsymbol{R}_0\boldsymbol{w}_i)\times[({}^i\boldsymbol{R}_0\boldsymbol{w}_i)\times({}^i\boldsymbol{R}_0\bar{\boldsymbol{s}}_i^B)]\\&+{}^i\boldsymbol{R}_0\dot{\boldsymbol{v}}_{i-1}\end{aligned} \tag{32}$$

where $\bar{\boldsymbol{s}}_i^A$ and $\bar{\boldsymbol{s}}_i^B$ are vectors representing distances of sensor system A and B from the rotational center and satisfying

$$\bar{\boldsymbol{s}}_i^B=\bar{\boldsymbol{s}}_i^A+\bar{\boldsymbol{p}}_i^{AB}, \tag{33}$$

where $\bar{\boldsymbol{p}}_i^{AB}$ is a known constant vector. Then from the above two equations, we get:

$$\begin{aligned}{}^i\boldsymbol{R}_0\bar{\boldsymbol{a}}_i^B-{}^i\boldsymbol{R}_0\bar{\boldsymbol{a}}_i^A=&({}^i\boldsymbol{R}_0\dot{\boldsymbol{w}}_i)\times({}^i\boldsymbol{R}_0\bar{\boldsymbol{p}}_i^{AB})+({}^i\boldsymbol{R}_0\boldsymbol{w}_i)\times[({}^i\boldsymbol{R}_0\boldsymbol{w}_i)\\&\times({}^i\boldsymbol{R}_0\bar{\boldsymbol{p}}_i^{AB})]\stackrel{\text{def}}{=}{}^i\boldsymbol{R}_0\bar{\boldsymbol{a}}_i^p.\end{aligned} \tag{34}$$

Since ${}^i\boldsymbol{R}_0\dot{\boldsymbol{w}}_i=[0 \;\; 0 \;\; \| \; {}^i\boldsymbol{R}_0\dot{\boldsymbol{w}}_i \; \|]^T$ and ${}^i\boldsymbol{R}_0\dot{\boldsymbol{w}}_i=[0 \;\; 0 \;\; \| \; {}^i\boldsymbol{R}_0\boldsymbol{w}_i \; \|]^T$, we know the relation between ${}^i\boldsymbol{R}_0\bar{\boldsymbol{a}}_i^A$ and ${}^i\boldsymbol{R}_0\bar{\boldsymbol{p}}_i^{AB}$. Let's denote the relation as ${}^i\boldsymbol{R}_z(\theta)$ there θ is the rotation angle by which we can align the two vectors. Then, we get the following equation:

$$\begin{aligned}&({}^i\boldsymbol{R}_0\dot{\boldsymbol{w}}_i)\times({}^i\boldsymbol{R}_0\bar{\boldsymbol{s}}_i^A)+({}^i\boldsymbol{R}_0\boldsymbol{w}_i)\times[({}^i\boldsymbol{R}_0\boldsymbol{w}_i)\times({}^i\boldsymbol{R}_0\bar{\boldsymbol{s}}_i^A)]\\&=\frac{\|\bar{\boldsymbol{s}}_i^A\|}{\|\bar{\boldsymbol{p}}_i^{AB}\|}\boldsymbol{R}_z(\theta){}^i\boldsymbol{R}_0\bar{\boldsymbol{a}}_i^p\end{aligned} \tag{35}$$

Since the terms on the right-hand side are all known or measurable, we determine the gravity-related term ${}^i\boldsymbol{R}_0\dot{\boldsymbol{v}}_{i-1}$ from (31). Then, we obtain the following equation through straightforward manipulation:

$${}^i\boldsymbol{R}_0\dot{\boldsymbol{v}}_{i-1}={}^i\boldsymbol{R}_{i-1}({}^{i-1}\boldsymbol{R}_0\dot{\boldsymbol{v}}_{i-1}). \tag{36}$$

Note that all of the matrices and variables on the left-hand side of equation (36) are determined from measurement or pre-defined kinematic relation, while the right-hand side has one unknown term ${}^i\boldsymbol{R}_{i-1}$ which is a function of the rotation angle about $(i-1)$ the joint. Note also that ${}^{i-1}\boldsymbol{R}_0\dot{\boldsymbol{v}}_{i-1}$ is calculated recursively. The equation (36) contains two unknown joint variables and is the same form as the equation (9) in Section 2. Hence, using equation (36), we can extract joint variables (actually body configuration) recursively through the same manner introduced in Section 2. In conclusion, if multiple sensor units are used, we can decompose two different kinds of accelerations (one from the motion of its own link and the other from the motion of previous link), and so we can extract relative body configuration even when the motional acceleration cannot be neglected.

Let's consider an example performed on a one degree of freedom motion (Figure 9). In this example, we made the link move along a sinusoidal angular velocity and the raw data is shown in Figure 8. Note that if the condition $\boldsymbol{\theta}_g \gg \boldsymbol{\theta}_a$ were satisfied, the data would be sinusoidal. Since the sensor data contains both a gravity term and motional term, it is far from a sinusoidal shape. After applying the technique described in this section, we decompose the two components and extract the joint variable as shown in Figure 10. From the figure we know that the proposed

https://doi.org/10.1017/S0263574701003319 Published online by Cambridge University Press

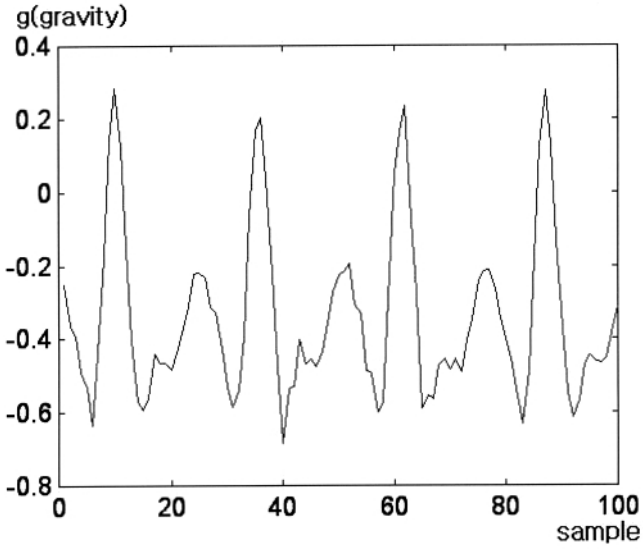


Fig. 8. Raw sensor data including gravity and non-gravity terms.

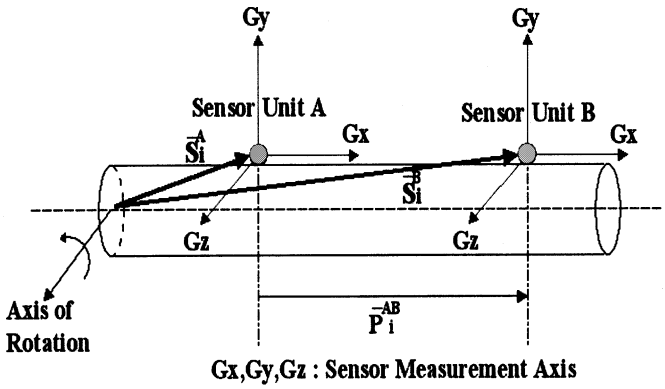


Fig. 9. Two sensor unit attached to link for compensating non-gravity term.

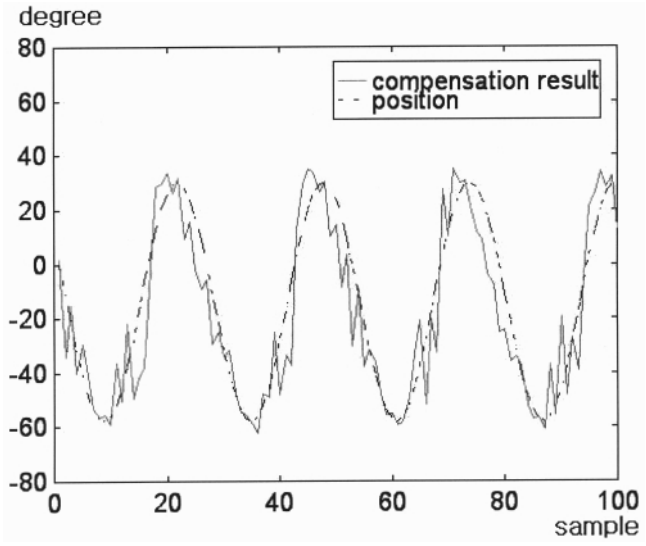


Fig. 10. Sensor information after compensating non-gravity term.

compensation technique make the processed data approach the true joint angle shown as a dotted line in the figure.

6. HUMAN BODY MOTION CAPTURING

To capture the motion of a human body, we modeled the human body into open-chained kinematic links that rotate about joints. In this experiment, we adopted a model proposed by Molet.[9] Joints with two degrees of freedom (for example, elbow and knee joints) are covered by one sensor unit that is composed of three accelerometers. Joints with three degrees of freedom (i.e. shoulder and neck joints) are covered by an electromagnetic compass[8] in addition to the sensor unit.

The overall system for real-time motion capturing is shown in Figure 2. An example of arm motion capturing is shown in Figure 11 and Figure 12. Figure 11 shows the sensory information calculated in real-time by the proposed techniques. In this experiment, the arm modeled two link system(shoulder and elbow) in two dimensional space: swings periodically so that we expect a sinusoidal data pattern for both the shoulder angle and the elbow angle. In the Figure, (a) shows the shoulder angle calculated directly from the sensory information (without compensation), which shows a sinusoidal pattern. This means the shoulder angle sensory information contains a negligible amount of motion acceleration compared to gravity acceleration. On the other hand, (b) shows the elbow angle calculated directly the sensory information, which is far from a sinusodal pattern. This may arise from the fact that, in this case, the elbow sensory information includes a non-negligible amount of motion acceleration in addition to the acceleration from gravity. To the data is applied the compensation algorithm explained in Section 5 so that we obtain the compensated sensory information of (c) which is described in a sinusoidal pattern. When we retrieve the actual arm motion from the selected part of the data (from 2,400 to 4,000 frames, 50 frames interval) (a) and (b), we

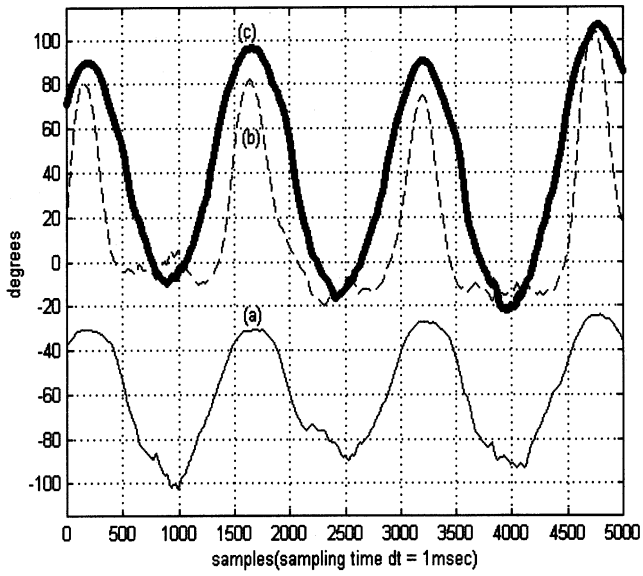


Fig. 11. Arm motion capturing example: (a) uncompensated sensory information of shoulder angle, (b) uncompensated sensory information of elbow angle, and (c) compensated sensory information for elbow angle.

https://doi.org/10.1017/S0263574701003319 Published online by Cambridge University Press

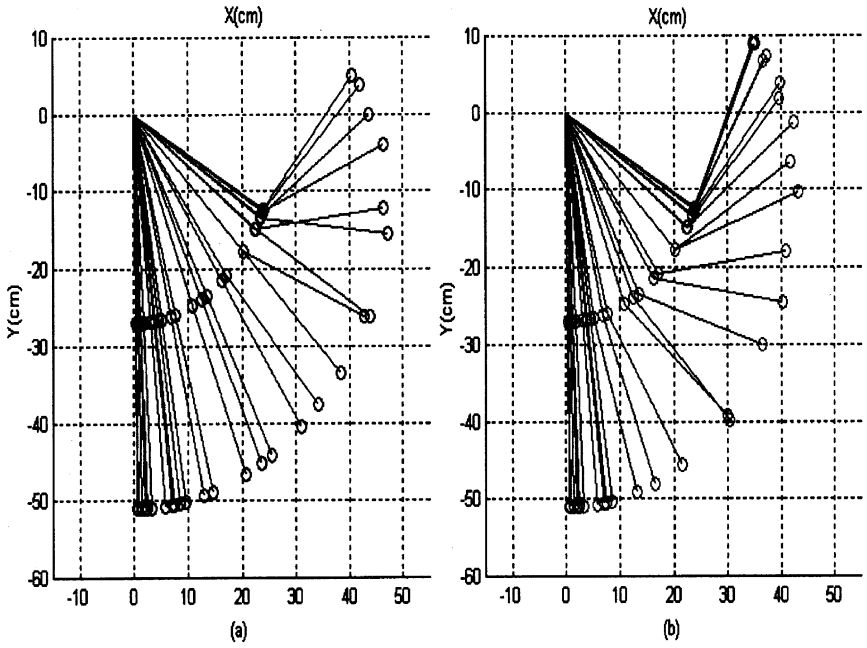


Fig. 12. (a) Arm motion reconstructed from Figure 11-(a) and (b). (b) Arm motion reconstructed from Figure 11-(a) asnd (c).

obtain the result shown in Figure 12-(a), while we obtain the arm motion 12-(b) from (a) and (c). Note that 12-(b) replicates the real experimental arm motion more precisely than 12-(a).

We also performed leg motion capturing experiments. The overall structure of the experiments are exactly the same as the arm motion experiments, and the results are shown in Figure 13 and Figure 14, which show the feasibility of the proposed technique.

More complex capturing examples for various parts of the human body are shown in Figures 15, 16 and 17, which include more complex arm, leg and head motion. One can find both the real character and modeled character on the monitor, which shows the motion capturing performed in a real-time manner.

7. CONCLUDING REMARKS

A technique that is capable of capturing human motion in real-time motion is proposed. The proposed system is mainly based on low cost accelerometers. The human body is modeled into a series of open-chained robots whose joints

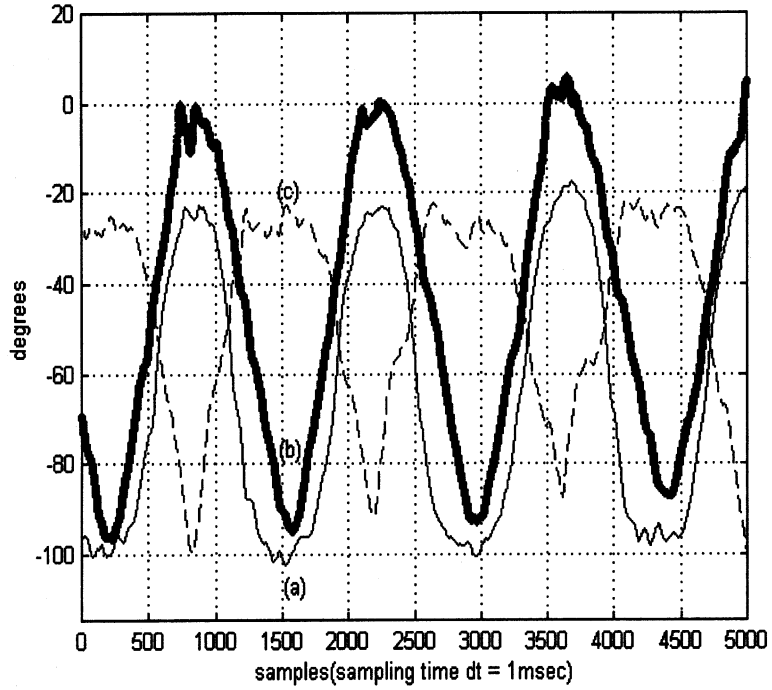


Fig. 13. Leg motion capturing example: (a) uncompensated sensory information of hip angle, (b) uncompensated sensory information of knee angle, and (c) compensated sensory information for knee angle.

https://doi.org/10.1017/S0263574701003319 Published online by Cambridge University Press

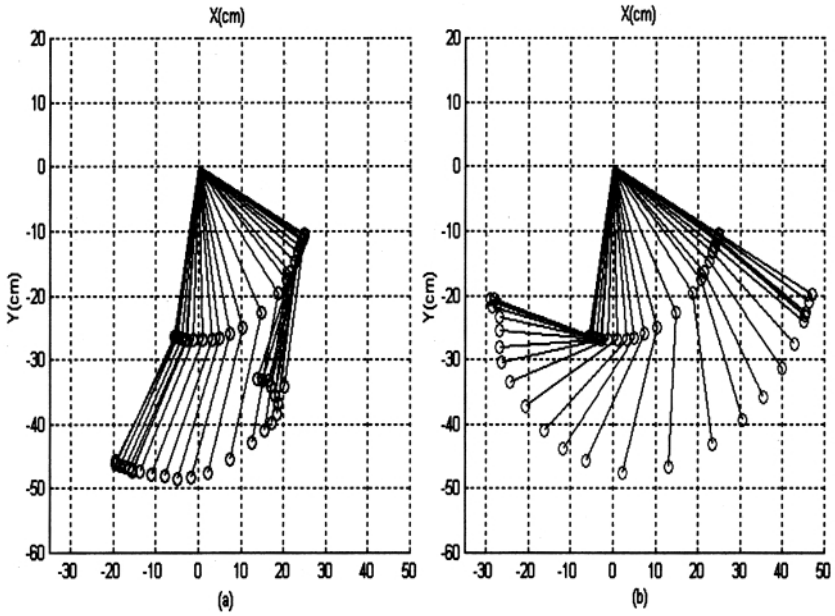


Fig. 14. Leg motion reconstructed from Figure 11-(a) and (b). (b) Leg motion reconstructed from Figure 11-(a) and (c).

have one, two, or three degrees of freedom. In addition to accelerometers, compasses are introduced to the human motion capture system in order to cover joints with more than 2 degrees of freedom.

The rotating angles of joints are extracted from the sensors and are refined through the sensor fusion technique. The gravity-related data of accelerometers is fused to reduce uncertainties through geometric optimization. Three sensors are combined into one sensor unit that covers two degrees of freedom of a rotating joint.

Even though the variance of sensor information is reduced by sensor fusion, the mean values of joint angles are strongly dependent on the calibration of the sensor system. Therefore, we propose a practical calibration method that can handle cases in which the sensing directions of each sensor are not orthogonal to each other. Additionally, since the proposed method is based on sensor data from gravity, some disturbances are introduced when the motion acclerations are not negligible. We propose a technique based on the redundant sensor system to decom-



Fig. 15. An example capturing human arm motion.

https://doi.org/10.1017/S0263574701003319 Published online by Cambridge University Press



Fig. 16. An example capturing human head motion.

pose the gravity term and the motion term. Applying the geometric sensor fusion and the calibration, we were able to successfully capture the human motion in real-time.

In the future, this technique should be extended to cases where the motions are faster than the case handled in this paper. In order to do so, we need to perform extensive

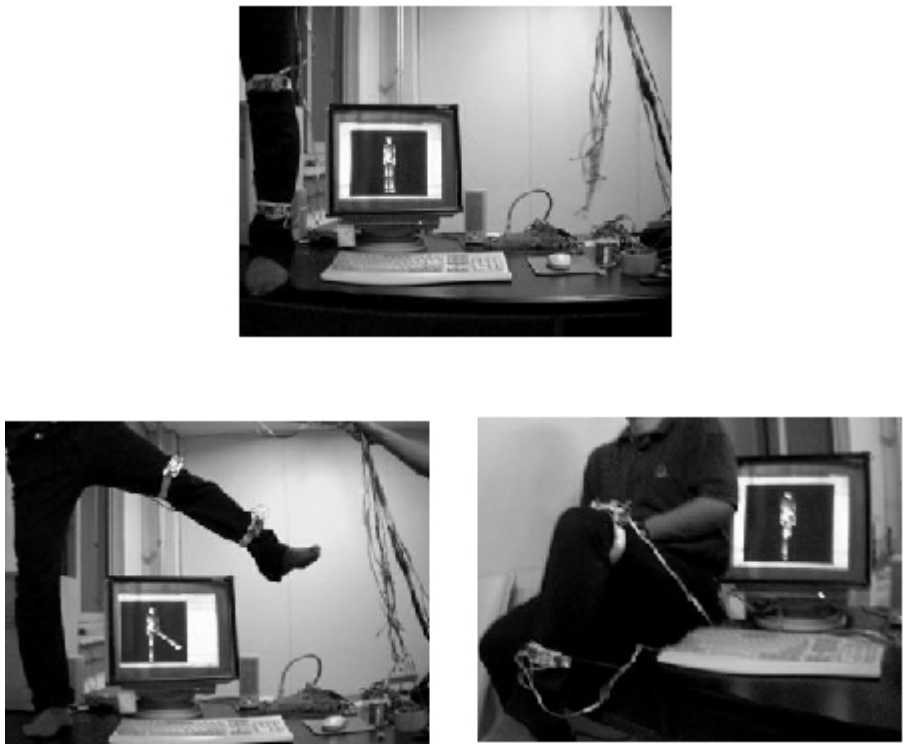


Fig. 17. An example capturing human leg motion.

https://doi.org/10.1017/S0263574701003319 Published online by Cambridge University Press

studies on extracting gravity-related term from sensor data in general cases. We believe that modeling the human body to a more complex structure and capturing the detailed motion requires much more extensive studies.

References

1. R. C. Luo and M. G. Kay, "Multisensor Integration and Fusion in Intelligent Systems", *IEEE Trans. on Systems, Man and Cybernetics*, **19**(No. 5), 901-931 (1989).
2. Y. Nakamura and Y. Xu, "Geometrical fusion method for multi-sensor robotic systems", *ICRA '94* (1994) pp. 668–673.
3. Y. Nakamura, *Advanced Robotics, Redundancy and Optimization* (Addison-Wesley Publishing Company).
4. S. Lee and S. Ro, "Uncertainty Self-Management with Perception Net Based Geometric Data Fusion", *ICRA '97* (1997) pp. 2075–2081.
5. I. Bloch, "Information Combination Operators for Data Fusion: A Comparative Review with Classification', *IEEE Trtans. on Systems, Man and Cybernetics*, **26**(No. 1), 52–67 (1996).
6. R. R. Murphy, "Biological and Cognitive Foundations of Intelligent Sensor Fusion", *IEEE Trans. on Systems, Man and Cybernetics*, **26**(No. 1), 42–51 (1996).
7. K. S. Fu, R. C. Gonzalez and C. S. G. Lee, *Robotics Control, Sensing, Vision and Intelligence* (McGraw-Hill, New York, 1987).
8. Precision Navigation, *Vector-2X Compass Module Application Notes. Version 1.0* (1995).
9. T. Molet, Z. Huang, R. Boulic and D. Thalmann, "An Animation Interface Designed for Motion Capture", *Proc. Computer Animation '97, IEEE CS Press* (1997) pp. 77–85.

https://doi.org/10.1017/S0263574701003319 Published online by Cambridge University Press